


Structural defects of monolayer wet particles during melting under vertical vibrationP. Kong ^{1,2} Peng Wang,^{2,3} Liang Zhou,¹ and Ran Li^{3,4,*}¹*Jiading District Central Hospital Affiliated Shanghai University of Medicine & Health Sciences, Shanghai 201800, China*²*Shanghai Key Laboratory for Molecular Imaging, Shanghai University of Medicine and Health Sciences, Shanghai 201318, China*³*School of Medical Instrument and Food Engineering, University of Shanghai for Science and Technology, Shanghai 200093, China*⁴*School of Optical-Electrical and Computer Engineering, University of Shanghai for Science and Technology, Shanghai 200093, China*

(Received 25 July 2021; accepted 14 December 2021; published 11 January 2022)

The evolution of structural defects during phase transition is of great significance to the understanding of the mechanism of solid-liquid transition. However, the current research on topological defects still uses the pair-correlation function and the orientational order correlation function, so it is difficult to quantify the detailed changes of structural defects locally. In this paper, the local volume fraction is proposed as a key parameter to accurately quantify the variation of structural defects. The experimental results indicate that the evolution of structural defects in the particle system is caused by the decrease of local volume fraction, so the critical value of phase transition could be determined by the minimum local volume fraction ϕ_{\min} . Furthermore, according to the evolution law of structural defects, it can be deduced that the phase transition is continuous, which is consistent with the Kosterlitz-Thouless-Halperin-Nelson-Young theory. Therefore, the quantitative analysis of structural defects by using local volume fraction can help make the mechanism of solid-liquid phase transformation clearer.

DOI: [10.1103/PhysRevE.105.014903](https://doi.org/10.1103/PhysRevE.105.014903)**I. INTRODUCTION**

The structural defects of wet particles and the critical states of phase transition during melting can provide valuable insights into the mechanism of two-dimensional solid-liquid transition [1–3]. Due to the presence of liquid-mediated capillary force between wet particles, agitated wet granular matter often behaves dramatically different from dry granular matter. Voronoi constructions in particle systems can be used to represent phase states [4]. Thus, the solid-liquid phase transformation process can be described according to the changes in the structural defects of particles in space. The Kosterlitz-Thouless-Halperin-Nelson-Young (KTHNY) theory predicted a two-stage continuous melting transition in 2D, from a quasi-long-ranged ordered solid to fluid via an intervening hexatic phase, which is induced by the formation of structural defects [5–8]. Many computer simulations and experimental studies have been conducted to determine phase transitions in two-dimensional solid particle system using positional correlation functions and structural factors [9–13]. However, these methods can only represent the phase transition as a whole, and it is difficult to quantitatively analyze the detailed changes of structural defects locally.

Recent studies have shown that the melting of two-dimensional particle system can be either continuous or discontinuous, depending on multiple parameters, such as particle stiffness, density, and particle size dispersion [12,14,15], etc. However, the fundamental reason is that the changes of external parameters lead to the changes of topological structure in the melting process. Therefore, it is a valuable research

orientation to explore the phase transformation in the melting process from the perspective of the changes of structural defects. Olafsen and Urbach [16] were the first to conduct an experimental study of the transition of a hexagonally ordered solid phase to a disordered liquid in the monolayer of a vibrating sphere. The results of the positional and the orientational correlation functions showed the evidence of a dislocation-mediated continuous transition from a solid phase with long-range order to a liquid with only short-range order. In the wet particle system, the collective behavior and interaction forms of the particle system are much more complex than those of the dry particle system due to the action of the liquid bridge force between particles [1]. Bossler and Koos [17] studied the influence of the capillary force of wet particles on the structure of particle clusters and proved that the topological structure of wet particles is affected by the capillary force. Ramming and Huang [18] studied the collective behavior of monolayer wet particles melting under vertical vibration, which was characterized by the structural form of the wet particles based on the bond order parameters, upon which they obtained data concerning the states of clustering, recombination, and melting, thus providing a theoretical basis for studying the structural defects of wet particles after aggregation. Although a large number of studies have been carried out on the solid-liquid melting phase transition in particle system [19–21], it is necessary to explore a more effective quantitative parameter if we want to explore the changes of structural defects in detail.

In this study, a quantitative research is carried out on the structural defects of monolayer wet particles in the solid-liquid melting process under vertical vibration. Section II describes the experimental system and research methods, and by using image-processing technology, the position of each

*kilzucard@163.com

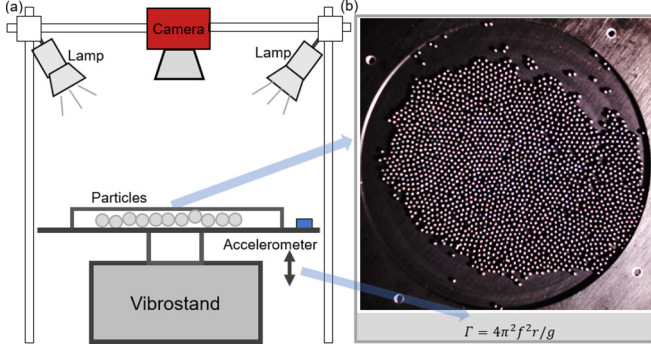


FIG. 1. Schematic of experimental setup. (a) A charge-coupled device is used to collect the data of the particles in the disk of the vertical vibrating table. (b) The camera captures the original images, in which each point of light is a particle.

particle is accurately located. Section III is an analysis and discussion of the experimental results. To be specific, firstly, the collective behavior of wet particle system is studied by using the bond orientation order parameter. Secondly, the Voronoi tessellations are established to investigate the changes of structural defects in the solid-liquid melting process of wet particle system. Thirdly, the evolution and critical value of structural defects are studied quantitatively by introducing local volume fraction. Finally, the credibility of the experimental results is verified by the probability distribution of the shape factor.

II. EXPERIMENT SYSTEM AND METHODS

A schematic of the experiment device is shown in Fig. 1. An electric vibration system is used on the vertical vibration table. The system is driven by sinusoidal signals generated by a frequency sweep generator (SA-SG030). The vibration parameters of the exciter (SA-JZ050) are adjusted by a power amplifier (SA-PA080), and the images are collected using a high-speed camera. The frequency f and amplitude r of the sinusoidal vibrations are recorded, and upon this, the dimensionless acceleration $\Gamma = 4\pi^2 f^2 r/g$ is calculated, where g represents the gravitational acceleration. Black glass beads with a diameter of $d = 2.0 \pm 0.02$ mm are used in the experiment and are mixed with a small amount of laboratory distilled water (LaboStar_TWF_7) and then are added to a cylindrical container made of fiberglass. The height is $H = 2.60 \pm 0.05$ mm, and the inner diameter is $D = 13.00$ cm; H should be only slightly larger than d to ensure that the particle system remains monolayer. The global area fraction is calculated using the equation $\varphi = Nd^2/D^2 \approx 50.6\%$, with the particle number $N = 2856$. The liquid content is defined as $W \equiv V_w/V_g$ [18], where V_w and V_g represent the volumes of liquid and glass beads, respectively. In the experiments, the amount of liquid added is approximately 3%, so that a liquid bridge could be formed between adjacent particles [22]. To maintain a constant liquid content during the experiment, a sealing ring is added around the disk to reduce the evaporation of water and ensure a constant liquid content.

To ensure repeatability of the experiments and to control the particles to cluster in the middle of the disk, we first

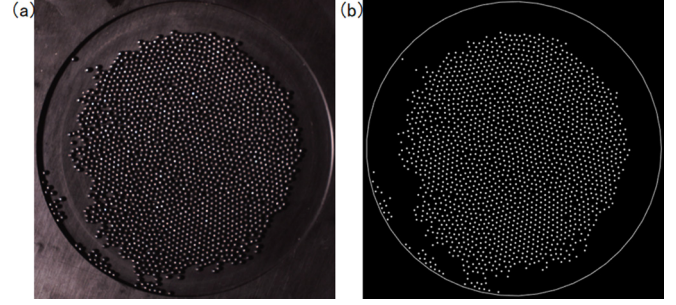


FIG. 2. Particle recognition and localization. (a) The original image; (b) the position of each particle obtained after image processing.

attached a water film to the middle part of the bottom wall of the container before loading the particles into the container. Then, the particles are placed in the container and the system acceleration is adjusted to $\Gamma \approx 20$. After running for 3 min, the particles basically gathered in the middle of the disk. Finally, Γ increases gradually from 0, and a camera is used to collect images of the particle system. In order to reduce the influence of vibration on the pixel of the particle image collected by the camera, we first determine the vibration frequency (vibration times per second) before the image acquisition, and then adjust the frame rate of the camera to be consistent with the vibration frequency.

In the process of image acquisition and processing, images acquire by the camera are denoised, binarized, and subjected to domain feature extraction to achieve the accurate identification of the white reflective spots in the picture. Then, a coordinate system is established with the lower-left corner of the image as the origin, and the position information of each particle is obtained, as shown in Fig. 2(b). To eliminate the positioning error caused by reflection on the water surface, the mutual position search algorithm is used to identify the distance between particles [23], and then it could be determined whether the white reflective spot is a particle.

Local symmetries of particle configurations are characterized with the bond orientational order parameters (BOOP) [24,25]. The formula calculation of BOOP is widely used in wet particle system at present [18]. The calculation method is simply as follows: from the particle positions, we can determine the connectivity of two particles with the criterion $|r_{ij}| \leq r_c$, where r_{ij} is the distance between the two particle centers, and the critical bond length $r_c = 1.15d$ is estimated from the rupture distance of a capillary bridge. It is defined as

$$Q_n = \sqrt{\frac{4\pi}{2n+1} \sum_{m=-n}^n |\bar{Q}_{nm}|^2}, \quad (1)$$

where $\bar{Q}_{nm} \equiv \langle Q_{nm}(\vec{r}) \rangle$ is an average of the local order parameter $Q_{nm}(\vec{r}) \equiv Y_{nm}(\theta_{ij}, \varphi_{ij})$ over all bonds connecting one particle to its nearest neighbors, with $Y_{nm}(\theta_{ij}, \varphi_{ij})$ spherical harmonics of a bond located at \vec{r} [23], where φ_{ij} is the azimuth and θ_{ij} is the polar angle ($\theta_{ij} = 0$ for the 2D case here). Here, we choose Q_6 as the order parameter because of its sensitivity to the hexagonal order. Compared with other local structure measurement methods (such as the coordination number and local area fraction), using BOOP parameter identification

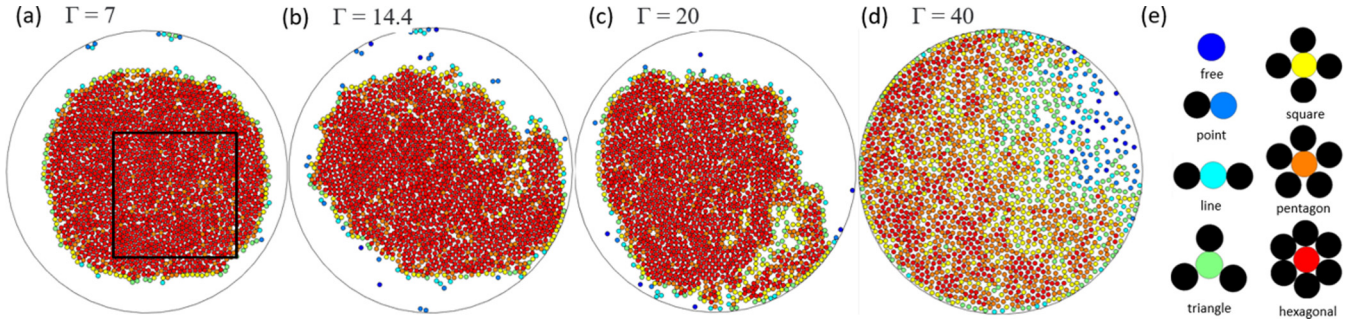


FIG. 3. The collective behavior of wet particle system under different dimensionless accelerations. Topological structure of particle system changes at (a) $\Gamma = 7$, (b) $\Gamma = 14.4$, (c) $\Gamma = 20$, and (d) $\Gamma = 40$. (e) Color coding for the local structure (free, line, square, or hexagonal) is identified by means of bond-orientational order parameters. Blue particles are free particles, yellow particles represent four bonds, and red particles represent hexagonal. In the particle system, the change in the particle structure is reflected as the phase change.

minimizes the influence of surrounding particles on the edge of the cluster, which is crucial for analyzing the structure of small clusters.

III. RESULTS AND DISCUSSION

A. The collective behavior and structural defect evolution

The collective behavior of a wet granular monolayer after agglomeration under different accelerations is identified by BOOP. Figure 3(a) shows the initial aggregation state of the experiment, in which the particle system is in a crystal-like state. In such a two-dimensional system, collisions are inelastic. A liquidlike steady state can be achieved only with constant external energy input. In principle, it is possible to drive the system uniformly throughout the container (uniform heating). In the experiment, however, the granular solids were driven by shaking the walls of the container. Such boundary heating method develops a gradient in density and in mean kinetic energy in the solids [26]. The effect of the topological structure on the positional ordering of the particles can be seen through the pair-correlation function $G(r) = \langle \rho(r')\rho(r'+r) \rangle / \langle \rho(r') \rangle^2$, where ρ is the particle density, $\rho(r')$ is the average particle number density at a distance from the reference particle r' . At the dimensionless acceleration $\Gamma = 0-14$, the positional correlations decay very slowly, consistent with an algebraic decay, as shown in Fig. 4(a). With the increase of Γ , the large cluster is locally fractured and decomposed to form small clusters, as shown in Figs. 3(b) and 3(c). This phenomenon is somewhat different from the surface melting previously studied [27]. This is because the effect of liquid bridge force makes the wet particle system more inclined to phase transition at the place with low liquid bridge force, rather than at the surface of the particle system. When Γ is higher, the relative separation distance between the two particles is greater than the rupture distance of the capillary bridge, and the particles are released from bondage and transform into a liquidlike form, as shown in Fig. 3(d). The positional order is clearly short ranged, and the system behaves as a disordered liquid. In condensed-matter physics, the collective behavior of the particle system is considered as a transition process from solid to liquid, during which structural defects and phase changes occur [28,29]. Next, we explored the physical mechanism of phase transitions by using

Voronoi tessellation to investigate the local changes of particle structural defects.

The Voronoi tessellations [16,30] are established according to the particles in the rectangular region shown in Fig. 3(a), and the formation and transformation of defects in the partial particle melting process are studied, as shown in Fig. 5. To identify various topological defects, we first obtain the coordination number n_v of each particle in the system by counting the number of its Voronoi neighbors. In a perfect hexagonal lattice $n_v = 6$ for all particles. We follow $n_v \neq 6$ particles to identify the n_v -fold defects. The red heptagon indicates that the particle topology is a sevenfold defect, and the blue pentagons indicates that the particle topology is a fivefold defect. The seven- and fivefold particles together constitute a defect [16], and multiple 5–7 defects combine to form a defect cluster [10].

To explore the evolution of structural defects, we calculate the number fraction of topological defects of various forms, as shown in Fig. 5(g). At $\Gamma = 14.4$, the right edge of the Voronoi cell begins to form five- to sevenfold structural defects; see Fig. 5(b). At the solid-hexatic transition, with the increase of Γ , the number fraction of 5–7 times defects begins to increase significantly, suggesting that the solid-hexatic transition is induced by the formation of five- to sevenfold defects. At $14.4 < \Gamma < 36$, the peak value of the pair-correlation functions of particles becomes smaller and the attenuation becomes faster, which is consistent with the results simulated by Jungmann *et al.* [31]. These phases are similar to the middle hexatic phase in the KTNHY theory. Although the system loses its angular order, it still maintains its radial interparticle constraint, which ultimately leads to melting. At a higher dimensionless acceleration, free disclinations are present [Fig. 5(e)], signifying the emergence of a disordered liquid. It is also interesting to note that five- to sevenfold defects begin to decrease after the appearance of free disclinations, and defect clusters increase sharply. More importantly, we find that the defect clusters (grain boundaries) fraction exceed the five- to sevenfold defects, indicating that the melting seems to be induced by a spontaneous proliferation of defect clusters instead of unbinding of dislocations and disclinations. It is also worth mentioning that both the fluid as well as the hexatic phase exhibit clear crystalline patches, which are surrounded by five- to sevenfold defects and defect clusters.

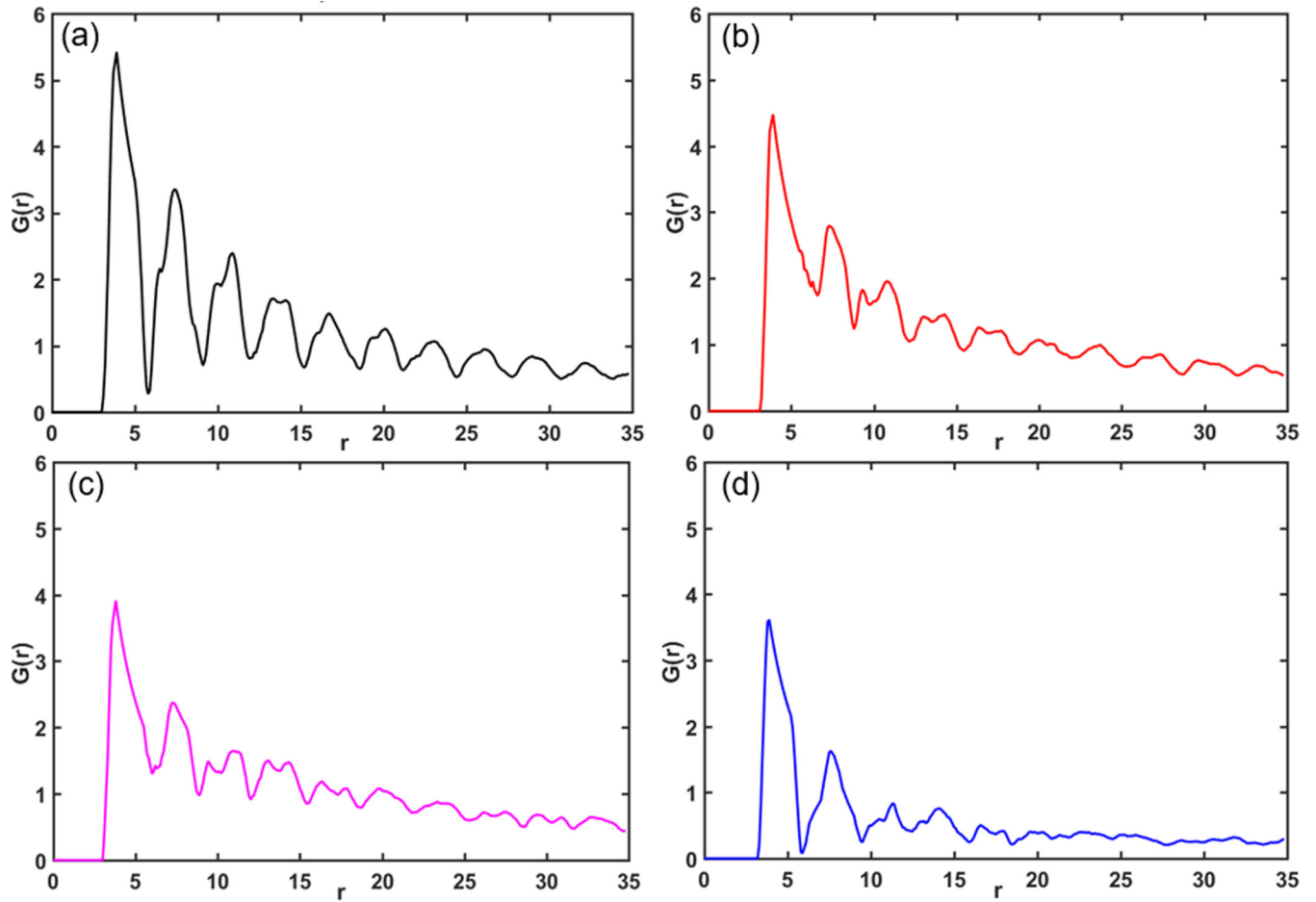


FIG. 4. Pair-correlation function for (a) $\Gamma = 7$, (b) $\Gamma = 14.4$, (c) $\Gamma = 20$, and (d) $\Gamma = 40$.

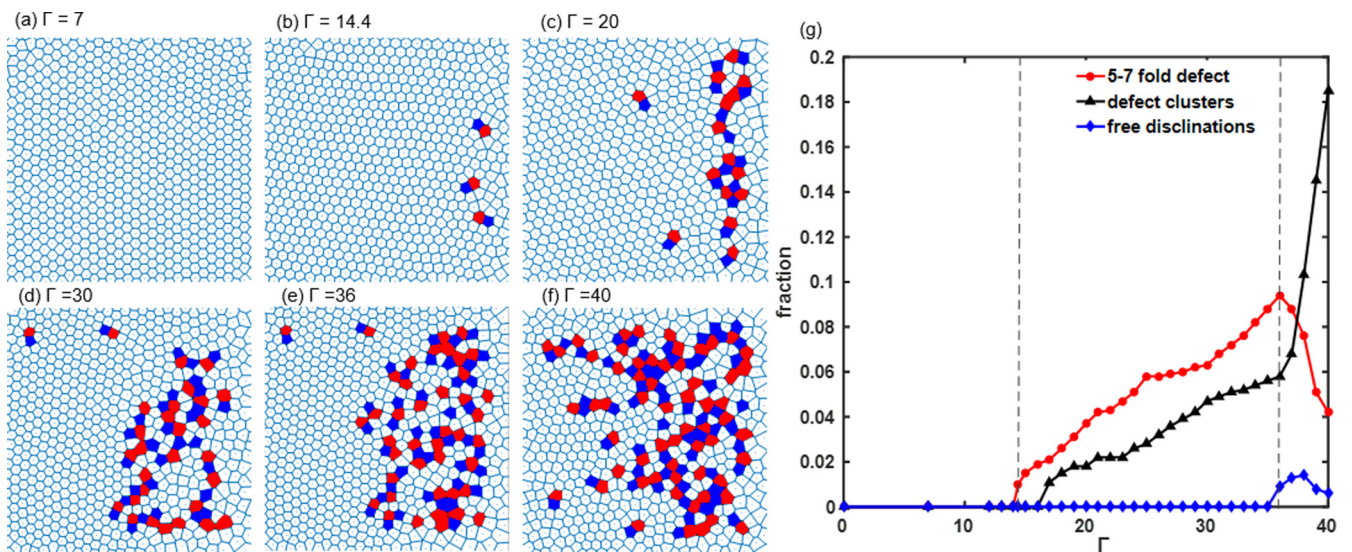


FIG. 5. The formation and evolution of defects during melting. Red heptagon (sevenfold) and blue pentagon (fivefold) together indicate a defect (five- to sevenfold). The isolated fivefold/sevenfold represents the free disclinations. (g) The number fraction change curve of five- to sevenfold defect (circles), defect clusters (triangles), and free disclinations (rhombus) under different accelerations. We define the number fraction as the number of respective defects divided by the total number of particles.

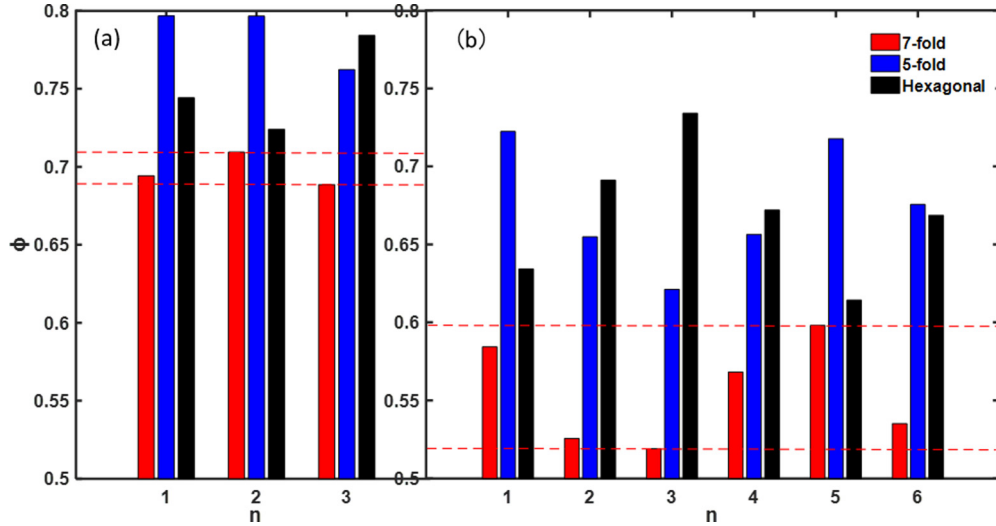


FIG. 6. The bar chart in (a) and (b) shows the local volume fraction of topologically defective particles in Figs. 5(b) and 5(c). The abscissa n represents the n th defect pair in Figs. 5(b) and 5(c). The red column represents the local volume fraction of sevenfold particles, the blue column represents the local volume fraction of fivefold particles, and the black column represents the local volume fraction of hexagonal before the occurrence of defects.

In the experiment, the melting is driven by an increase in the average kinetic energy of the particles as a result of the increase in vibration acceleration, suggesting a similar characteristic between particle temperature (δv^2) [32] and thermodynamic temperature. However, in the study of the nonequilibrium hard-sphere system, it is found that the particle temperature is not a relevant variable, and the phase transitions are driven by the density changes of the particle system [33]. In fact, a similar variable dominates the phase transitions in the melting process of a wet particle system as shown in Fig. 5. As the vibration acceleration increases, the monolayer particles begin to search for all available volumes within the finite disk space, resulting in changes in density. Therefore, the next section focuses on finding an appropriate variable to quantify such local density changes, so as to understand the critical state of solid-hexatic-liquid phase changes.

B. Quantitative analysis of structural defects

According to the geometric shape and area of the cell body in the Voronoi diagram, the topological changes of the particles are studied, and an improved Voronoi cell method is introduced to measure the local density of the particles. Voronoi cells are polyhedral and are closer to the locally movable space of particle i than other methods. According to the Voronoi cell method, the local volume fraction of particle i can be defined as [34]

$$\phi_i = \frac{V_i}{V_i^{\text{Voronoi}}}. \quad (2)$$

Here, V_i represents the volume of the i th particle, and V_i^{Voronoi} represents the volume of the polyhedron of the particle in the Voronoi diagram. The measurement of the local volume fraction of the particle system shows that the minimum local volume fraction of the system is consistent with the local volume fraction of the sevenfold defect when the defect occurs. Figures 6(a) and 6(b) show the local volume fraction

of structural defective particles in Figs. 5(b) and 5(c). The red and blue columns represent the local volume fraction of seven- and fivefold particles, while the black column represents the local volume fraction of hexagonal before the occurrence of defects. Interestingly, the local volume fraction of the particles with sevenfold defects is significantly smaller than that of the particles with fivefold defects and the hexagonal particles before structural defects. This further indicates that the minimum local volume fraction of the system is sevenfold defective particles. According to the study of Olafse and Urbach [16], the occurrence of five- to sevenfold defects indicates that the wet particle system enters the structural defect stage, and the occurrence of five- or sevenfold defects indicates that the particle system begins to convert to liquid. Therefore, the critical state of the phase transitions can be quantified by measuring the changes in the minimum local volume fraction in the particle system.

Figure 7 shows the changes in the minimum local volume fraction (ϕ_{\min}) and the average local volume fraction (ϕ_{mean}) in the particle system under different vibration accelerations. The red curve represents the changes of ϕ_{\min} and ϕ_{mean} when water content $W = 2\%$. The phase diagram of the granular system under this moisture content is shown in Fig. 5. This distribution of data values is represented by showing a single data point, representing the mean value of the data, and error bars to represent the overall distribution of the data. The error bars are represented by the standard deviation of the mean, often called the standard error. The standard error is calculated by dividing the standard deviation by the square root of number N of measurements that make up the mean (the experimental results are calculated through $N = 5$ experiments). As long as the fluctuation of the critical value is within the error bar, the critical value is acceptable.

The local volume fraction at $\Gamma = 0$ is the initial aggregation state of the experiment, which is obtained after adjusting the acceleration of the system to $\Gamma \approx 20$ and running for 3 min. The initial aggregation state of the system is not

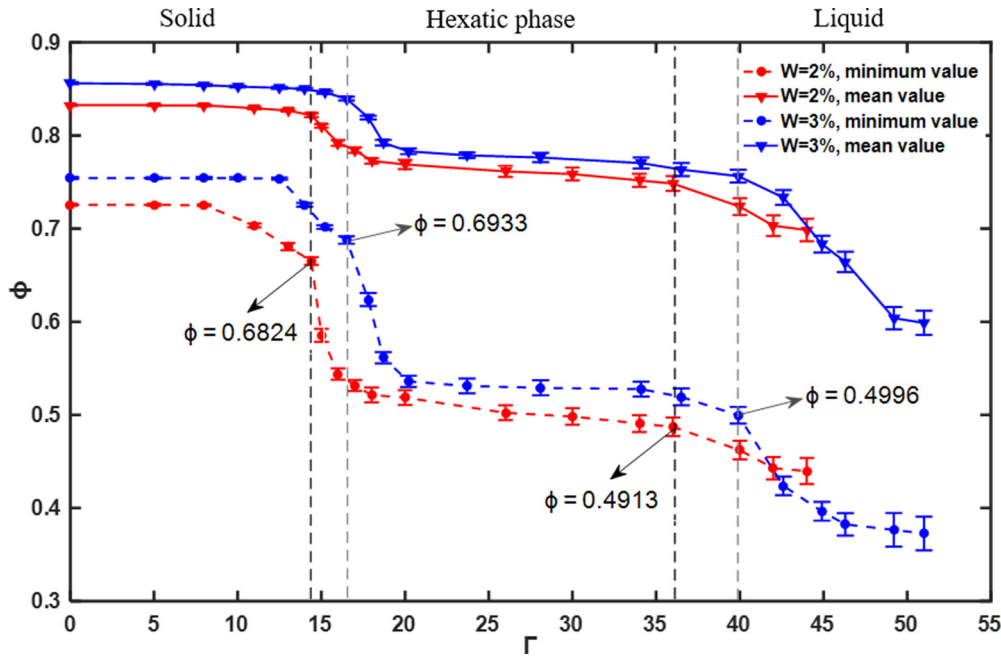


FIG. 7. The curve shows the variation trend of ϕ_{\min} and ϕ_{mean} in the particle system is under different vibration accelerations when water content $W = 2\%$ and $W = 3\%$. The dashed lines represent the minimum local volume fraction of the particle system under different accelerations, and the full line represents the average local volume fraction of all the particles in the system. The critical local volume fraction is determined according to the phase transitions under different accelerations, and the phase transitions during the melting process are quantitatively studied.

the most dense, but the structure arrangement of the particle system reaches the crystal-like structure. Under the same vibration condition, increasing water content will increase the liquid bridging force between particles, which will lead to more dense particle clusters. Therefore, at $\Gamma = 0$, $W = 3\%$, the local volume fraction of the granular system is larger than that at $W = 2\%$. At $\Gamma < 8$, the vibration intensity is low; thus, the particle system is almost in a stationary state. Moreover, the local volume fraction of the particles remains unchanged at this stage. At $8 < \Gamma < 14.4$, the wet particle system fluctuates as a whole as a large crystal cluster, but owing to the liquid bridge force, the particle system maintains in a stable state. At $\Gamma < 14.4$, the wet particle system appears as a solid phase characterized by algebraically decaying positional order. At $\Gamma = 14.4$, as indicated by the Voronoi cell [Fig. 5(b)], that five- to sevenfold structural defects begin to appear in the right edge of the Voronoi cell. The minimum local volume fraction is $\phi_{\min} = 0.6824$, and from that point it drops sharply. According to the changes of phase diagram in Fig. 5, it can be concluded that the wet particle system begins to transition from solid phase to hexatic phase when $\phi_{\min} = 0.6824$, and the transition is caused by the generation of five- to sevenfold structural defects. At $14.4 < \Gamma < 36$, the local volume fractions of particles significantly decrease and then reach a stable state, and the attenuation trend is exponential. These phase diagrams of this region show a typical hexatic phase. At $\Gamma = 36$, the attenuation of the minimum local volume fraction of the particle system becomes faster again, corresponding to the isolated sevenfold or fivefold defects in Fig. 5(e). At this time, the minimum local volume fraction $\phi_{\min} = 0.4913$, the particle system begins to undergo a transition from hexatic phase to liquid phase by the unbinding of disclination pairs.

The topological structure of the whole particle system is disorderly, which is consistent with the results of Fig. 5.

According to the variation trend of local volume fraction under different water content in Fig. 7, three phenomena come into our view: First, the increase of water content can increase the local volume fraction of particles. This is because the presence of liquid on the surface of particles increases the cohesion between particles, leading to the decrease of local free space of particles. Second, the critical value of the structure defect is obviously shifted to the right. The reason is that the particle movement requires greater energy to overcome the resistance due to the increase of the liquid bridge force. It can also be found that the structural changes of the particle system under the action of liquid bridge force are more complex compared with the research of Reis *et al.* [35]. The increase of the external driving force enables particles to overcome friction so that the “crystal” moves. As the interaction between the particles on the surface of the crystal is weak, the particles on the surface of the crystal become sparse, resulting in structural defects, and diffuse to the loose area of the internal structure of the crystal. Third, the local volume fraction of particles does not mutate when structural defects are produced, but decreases slightly before defects are produced. The phenomenon indicates that the phase transition in solid-liquid melting process is continuous, which is consistent with the phase transformation continuity in KTHNY theory.

C. Probability distribution statistics of shape factor

To verify that the local volume fraction can effectively quantify the variation of structural defects, the probability distribution of the shape factor is calculated. Shape factor is

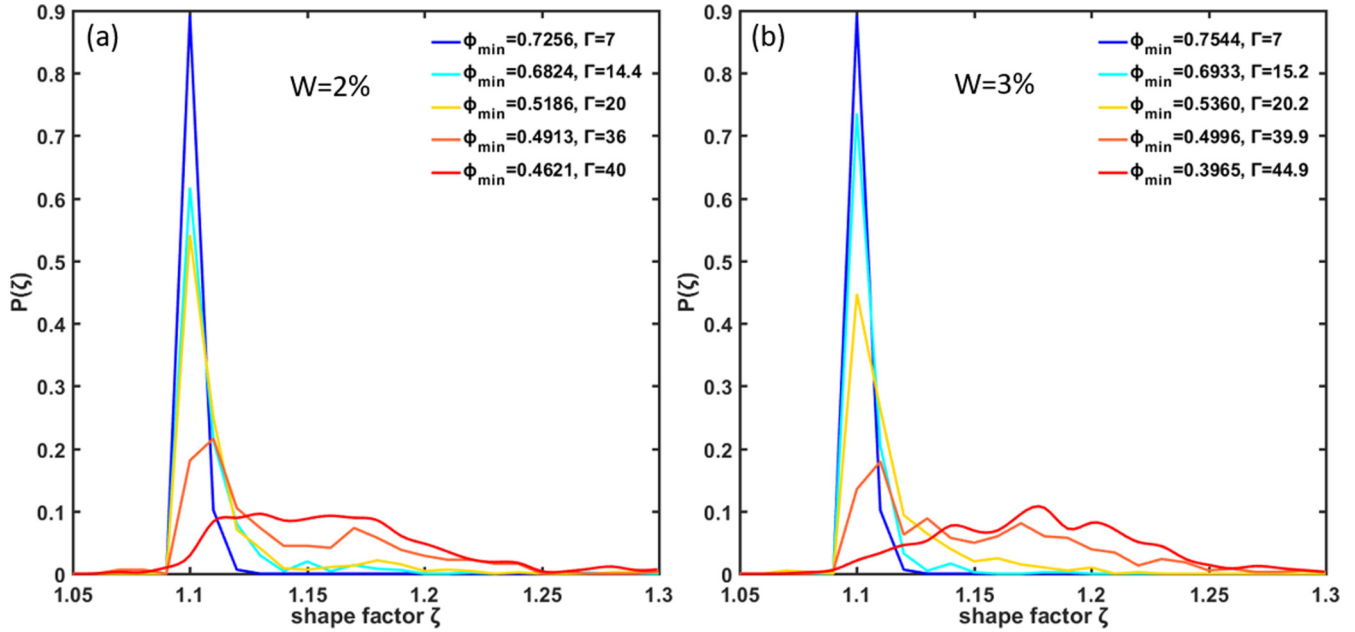


FIG. 8. Probability distribution of shape factor under different accelerations when water content $W = 2\%$ and $W = 3\%$. (a) The corresponding phase diagram is shown in Fig. 5.

a dimensionless parameter that measures the degree to which Voronoi cells deviate from the round shape. The distribution of shape factors clearly indicates that there are different potential substructures (domains) in the particle system. To verify the reliability of the critical value of the phase transitions obtained by using ϕ_{\min} , the probability $P(\zeta)$ distribution of the shape factor at different local volume fractions in the phase diagram in Fig. 5 is statistically analyzed. This variable is used to quantify the local structure of the particle by Voronoi diagram, which is defined [36] as $\zeta = \frac{C^2}{4\pi S}$, where C is the perimeter of the polygon in the Voronoi diagram, and S is the area of the polygon in the Voronoi diagram. By cell measurement of different shapes, the distribution law of shape factors is obtained. For circles $\zeta = 1$ and for all other shapes $\zeta > 1$. For a square $\zeta = 1.273$, for regular pentagons $\zeta = 1.156$, and for regular hexagons $\zeta = 1.103$. The shape factor combines the perimeter and the surface, so it is sensitive to the changes of two-dimensional structure and can clearly identify the potential changes of structure. Therefore, the shape factor recognition of Voronoi cells is used to verify the critical value of phase transition obtained by using the ϕ_{\min} .

Figure 8 shows the probability distribution curve of shape factor under different water content. Figure 7(a) is the probability distribution curve of shape factor at different ϕ_{\min} when water content $W = 2\%$, and the corresponding phase diagrams is shown in Fig. 5. At low dimensionless acceleration, the distribution of cell shape factors is concentrated at $\zeta = 1.103$ and has a unique peak value. The Voronoi cells show a regular hexagonal crystal structure. As the acceleration increases, a small peak can be observed in the probability distribution curve at $\phi_{\min} = 0.6824$. It shows that when $\phi_{\min} = 0.6824$, the phase diagram of the particle system has structural defects, and the particle system begins to undergo solid-hexatic phase transition. At the stage $14 < \Gamma < 36$, the first peak in the probability distribution curve becomes smaller

and shifts to the right, while the second peak becomes larger and the whole curve shifts to the right, indicating that the structural defects in the wet particle system further expand. The variation of the probability distribution of the shape factor under different accelerations is consistent with the variation of the minimum local volume fraction, which once again proves that the local volume can be used as a key parameter to quantify structural defects. At higher accelerations, the peak of the probability distribution curve becomes flat and the first peak gradually disappears, indicating that the structure of the particles in the particle system is gradually disordered and the phase diagram is transformed from hexatic phase to liquid.

By comparing the shape factor distribution curves of the particle system under different water content, it is found that the trend of the probability distribution curves of the shape factor under different water content is roughly the same. The difference is only in the increase of acceleration as structural defects are produced, which is consistent with the results obtained by using local volume local fraction.

IV. CONCLUSIONS

In summary, we have quantitatively studied the structural defects of monolayer wet particles during melting under vertical vibration. Firstly, a study of the collective behavior of the granular system shows that melting is more likely to occur in the region with low liquid bridge force than on the surface of the granular system due to the action of liquid bridge force. According to the phase diagram evolution and the statistics of structural defects, the melting seems to be induced by a spontaneous proliferation of defect clusters instead of the unbinding of dislocations and disclinations. Secondly, by introducing the parameter of local volume fraction ϕ_i , the changes of structural defects are measured in detail. The experimental results indicate that the evolution of structural

defects is caused by the decrease of local volume fraction during phase transition. In the particle system, the critical value of phase transitions can be determined according to the change curves of the minimum local volume fraction, which is sevenfold defect. The change curves of the minimum local volume fraction show that the structural defects are not abrupt and the phase transition is continuous, which is consistent with the KTHNY theory. Finally, the reliability of the critical value of phase transitions obtained by the minimum local volume fraction is verified by the probability distribution of the shape factor.

In the future study of condensed-matter structure of two-dimensional melting system, the constraint of using only correlation function (the pair-correlation function and the orientational order correlation function) can be broken, and the evolution of structure can be quantified by using local volume fraction. The local free space of particles can be accurately quantified by using the local volume fraction, so that small changes in local density of particles can be obtained in experiments. At present, the collective behavior and structural evolution of two-dimensional melting are well quantified, but

the physical mechanism of structural defects during solid-liquid phase transformation is still controversial. Therefore, future research should focus on the study of dislocation and disorientation in the phase transformation process, and quantitative study of the physical mechanism of the occurrence and transformation of structural defects.

ACKNOWLEDGMENTS

The project was supported by the National Natural Science Foundation of China (Grant No. 11902190), the Construction Project of Shanghai Key Laboratory of Molecular Imaging (Grant No. 18DZ2260400), and the Fund from the Shanghai Municipal Education Commission, China (Class II Plateau Disciplinary Construction Program of Medical Technology of SUMHS, 2018–2020). We would like to express our gratitude to Prof. Kai Huang from Duke Kunshan University for his careful guidance and help, and Prof. Hui Yang from School of Optoelectronic Information and Computer Engineering, University of Shanghai for Science and Technology, for his experimental equipment and support.

-
- [1] S. Herminghaus, *Soft Matter* **8**, 8271 (2012).
 - [2] J. Li, Y. Cao, C. Xia, B. Kou, X. Xiao, K. Fezzaa, and Y. Wang, *Nat. Commun.* **5**, 5014 (2014).
 - [3] F. Alarcón, C. Valeriani, and I. Pagonabarraga, *Soft Matter* **13**, 814 (2017).
 - [4] M. Mazars, Melting in monolayers: Hexatic and fluid phases, [arXiv:1301.1571](https://arxiv.org/abs/1301.1571).
 - [5] J. M. Kosterlitz and D. J. Thouless, *J. Phys. C* **6**, 1181 (1973).
 - [6] B. I. Halperin and D. R. Nelson, *Phys. Rev. Lett.* **41**, 121 (1978).
 - [7] D. R. Nelson and B. I. Halperin, *Phys. Rev. B* **19**, 2457 (1979).
 - [8] A. P. Young, *Phys. Rev. B* **19**, 1855 (1979).
 - [9] S. Deuschländer, T. Horn, H. Löwen, G. Maret, and P. Keim, *Phys. Rev. Lett.* **111**, 098301 (2013).
 - [10] W. Qi, A. P. Gantapara, and M. Dijkstra, *Soft Matter* **10**, 5449 (2014).
 - [11] G. Castillo, N. Mujica, and R. Soto, *Phys. Rev. E* **91**, 012141 (2015).
 - [12] S. C. Kapfer and W. Krauth, *Phys. Rev. Lett.* **114**, 035702 (2015).
 - [13] T. Schindler and S. C. Kapfer, *Phys. Rev. E* **99**, 022902 (2019).
 - [14] E. P. Bernard and W. Krauth, *Phys. Rev. Lett.* **107**, 155704 (2011).
 - [15] J. Guo, Y. Nie, and N. Xu, *Soft Matter* **17**, 3397 (2021).
 - [16] J. S. Olafsen and J. S. Urbach, *Phys. Rev. Lett.* **95**, 098002 (2005).
 - [17] F. Bossler and E. Koos, *Langmuir* **32**, 1489 (2016).
 - [18] P. Ramming and K. Huang, *EPJ Web Conf.* **140**, 08003 (2017).
 - [19] S. C. Tai and S. S. Hsiau, *Powder Technol.* **194**, 159 (2009).
 - [20] A. E. Lobkovsky, F. V. Reyes, and J. S. Urbach, *Eur. Phys. J.: Spec. Top.* **179**, 113 (2009).
 - [21] S. Weis, G. E. Schröder-Turk, and M. Schröter, *New J. Phys.* **21**, 043020 (2019).
 - [22] V. A. Levashov, R. Ryltsev, and N. Chtchelkatchev, *Soft Matter* **15**, 8840 (2019).
 - [23] C. Lei and J. Ruan, *BioData Mining* **3**, 9 (2010).
 - [24] K. Huang, *New J. Phys.* **17**, 083055 (2015).
 - [25] L. Agosta, A. Metere, and M. Dzugutov, *Phys. Rev. E* **97**, 052702 (2018).
 - [26] Y. Chen, M. Hou, P. Evesque, Y. Jiang, and M. Liu, in *Powders and Grains 2013: Proceedings of the 7th International Conference on Micromechanics of Granular Media*, edited by A. Yu, K. Dong, R. Yang, and S. Luding, AIP Conf. Proc. No. 1542 (AIP, New York, 2013), p. 791.
 - [27] C. May, M. Wild, I. Rehberg, and K. Huang, *Phys. Rev. E* **88**, 062201 (2013).
 - [28] D. Risso, S. Rodrigo, and M. Guzmán, *Phys. Rev. E* **98**, 022901 (2018).
 - [29] L.-H. Luu, G. Castillo, N. Mujica, and R. Soto, *Phys. Rev. E* **87**, 040202(R) (2013).
 - [30] T. Aste and D. Weaire, *The Pursuit of Perfect Packing* (Institute of Physics Publishing, Bristol, 2000).
 - [31] R. M. Jungmann, P. C. N. Pereira, and S. W. S. Apolinario, *J. Phys.: Condens. Matter.* **30**, 465402 (2018).
 - [32] H. Yang, Y. Zhu, R. Li, and Q. Sun, *Particuology* **48**, 160 (2020).
 - [33] G. Castillo, N. Mujica, and R. Soto, *Phys. Rev. Lett.* **109**, 095701 (2012).
 - [34] J. J. Williamson and R. M. L. Evans, *J. Chem. Phys.* **141**, 164901 (2014).
 - [35] P. M. Reis, R. A. Ingale, and M. D. Shattuck, *Phys. Rev. Lett.* **96**, 258001 (2006).
 - [36] D. Dujak, A. Karač, Z. Jakšič, D. Vasiljević, and S. Vrhovac, *Sci. Tech. Rev.* **64**, 13 (2014).